Available online at www.sciencedirect.com
SCIENCE DIRECT
Tetrahedron
Tetrahedron 62 (2006) 5962–5972

Conformationally restricted triplex-forming oligonucleotides (TFOs). Binding properties of α-L-LNA and introduction of the N^7-glycosylated LNA-guanosine

Alexei A. Koshkin*

Exiqon A/S, Department of Chemistry, Bygstubben 9, DK-2950 Vedbæk, Denmark

Received 17 January 2006; revised 23 March 2006; accepted 6 April 2006
Available online 3 May 2006

Abstract—The method for scaled-up production of α-L-LNA phosphoramidite building blocks containing thymine and 5-methylcytosine nucleobases is described. Binding properties of pyrimidine TFOs modified with α-L-LNA are reported. In contrast to LNA TFOs, the fully modified α-L-LNA forms a stable triplex with a model DNA duplex. Pyrimidine DNA/LNA/α-L-LNA chimeras also efficiently hybridize with a model DNA duplex in the parallel mode. LNA nucleoside containing unnatural N^7-glycosylated guanine (LNA-^{7}G) was synthesized by a convergent method and incorporated into LNA oligonucleotides. The triplex-forming alternating DNA/LNA oligonucleotides containing a single LNA-^{7}G modification instead of internal LNA-mC demonstrate improved pH-dependent properties. The single LNA-^{7}G modification can also discriminatively reduce competitive binding of TFOs to natural nucleic acids in the antiparallel duplex mode.

1. Introduction

The design of molecules that can specifically recognize the DNA double helix would provide a means to interfere with gene expression at an early stage, thus giving tools for a wide range of applications in gene-based biotechnology and therapeutics. One approach for specific recognition of predetermined DNA sequences is based on triple helix formation, which is the phenomenon of third oligonucleotide strand (triplex-forming oligonucleotide, TFO) binding to a specific target site in duplex DNA.[1–3] It has been found that TFOs bind in the major groove of oligopyrimidine–oligopurine sequences in duplex DNA by hydrogen bonding with purine bases to produce base triplets in a sequence-specific manner.[4] Two main structural motifs have been established in which a TFO binds either in a parallel or antiparallel fashion respective to the target purine strand. Parallel triplexes contain C^+·GC and T·AT triplets[5] and have attracted much attention due to their comparatively high stability under physiological conditions. The fact that TFOs can only bind to oligopurine–oligopyrimidine target strands results in a major limitation to the application of TFOs. However, the recent in silico analysis of the human genome[6] has revealed that regions likely to form triplexes are more common than predicted by random models. The population of TFO target sequences is large in all the genome, without major differences between chromosomes. Moreover, the largest concentration of such sequences has been found in regulatory regions, especially in promoter regions, suggesting a tremendous potential for triplex technology.[6]

Much research on exploiting TFO binding in vivo has been reviewed recently.[7–9] However, there are still limitations to the use of TFOs. These concern binding affinity and specificity, uptake into cells and tissues, and in vivo stability. Major efforts have been devoted to improving TFO characteristics through chemical modifications. Thus, large variety of modifications to the TFO backbone has been attempted in order to increase the general affinity of the TFO to duplex DNA and its stability in vivo. The structures of the most promising TFO analogues with modified backbone are depicted in Figure 1. In the case of peptide nucleic acids (PNA), the whole phosphodiester backbone is replaced by an uncharged polyamide backbone.[10,11] The triplex-forming feature of PNAs has been described to lie in recognition of the DNA duplex via a strand invasion mechanism.[12,13] Cellular uptake of PNAs, however, still raises major problems and needs to be improved in order to fully exploit their properties.[14]

N3′–P5′ phosphoramidate TFOs (Fig. 1) have been demonstrated to bind strongly to double-stranded DNA.[15,16] It appears that this class of modified oligonucleotides has a favorable intracellular and tissue distribution, which makes them good candidates for in vivo applications.[16,17] The replacement of the 3′-oxygen atom by nitrogen, made in N3′–P5′ phosphoramidates in comparison to DNA, results in a substantial change of the sugar conformation. The

Keywords: LNA; α-L-LNA; N^7-Glycosylated guanine; Triplex-forming oligonucleotides.
* Tel.: +45 45650429; fax: +45 45661888; e-mail: koshkin@exiqon.com

0040–4020/$ - see front matter © 2006 Elsevier Ltd. All rights reserved.
doi:10.1016/j.tet.2006.04.016

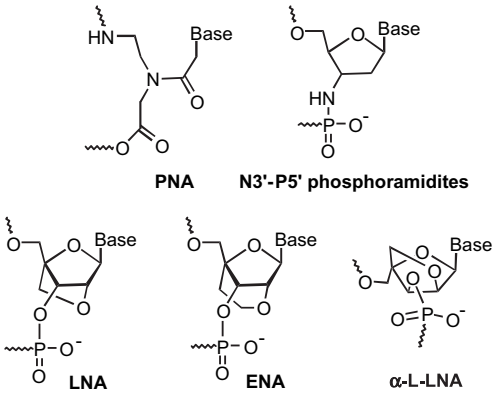

Figure 1. Molecular structures of selected TFOs with modified backbone.

resulting N-type conformation[18] may give an explanation for enhanced triplex-forming ability.

Modifications made to the ribose moiety in TFOs have also been able to generate derivatives with advantageous properties. Thus, locked nucleic acid (LNA) and 2′-*O*,4′-*C*-ethylene-briged nucleic acid (ENA) are RNA derivatives in which the ribose unit is constrained by a methylene or an ethylene linkage between the 2′-oxygen and the 4′-carbon (Fig. 1). This bridge reduces the conformational flexibility of the ribose and thus results in a locked 3′-*endo* (N-type) sugar puckering.[19–21] Along with N3′–P5′ phosphoramidates, the outstanding results on binding properties of LNA and ENA have clearly demonstrated that such restriction of the sugar conformation is a very promising approach for TFOs design.[21,22] Accordingly, TFOs consisting of alternating LNA and DNA residues have demonstrated significantly enhanced affinity to dsDNA with respect to the isosequential DNA TFOs.[21] The NMR structure of an LNA·dsDNA triplex has been determined recently.[23] The triplex has a regular seamless structure despite the fact that the TFO strand is composed of DNA and LNA monomers with different sugar puckers. The structure of the DNA duplex is changed to fit TFO accommodation, and it adopts a geometry intermediate between A and B types.

It has been found that ENA TFOs (Fig. 1) form stable triplexes with dsDNA similar to those partially modified with LNA nucleosides.[22] Furthermore, in contrast to LNA, fully modified ENA oligonucleotides have high triplex formation ability. Additionally, ENAs are generally more nuclease resistant than LNAs and, as a result, have greater potential for in vivo applications.[20,22] However, the availability of ENA is still comparatively limited as its synthesis, reported hitherto,[20] is significantly more resource consuming than that for LNA.[24]

Bearing in mind the achievements in constructing conformationally constrained TFOs, we report herein the results of our investigations into the binding properties of TFOs modified with α-L-*ribo*-configured locked nucleic acid (α-L-LNA; Fig. 1). The first synthesis and some properties of α-L-LNA have been recently reported.[25,26] The binding studies have demonstrated high affinity Watson–Crick hybridization between α-L-LNA and single stranded DNA oligonucleotides.[25] Interestingly, NMR studies have revealed that, in general, α-L-LNA nucleosides do not perturb native B-like dsDNA geometry.[27] In other words, when incorporated into the DNA duplex, they acted in a similar way to the fixed *S*-type sugar conformers despite their unnatural stereochemistry. Based on these findings, we anticipated that TFOs modified with α-L-LNA would form, if any, very structurally distinctive triplexes with dsDNA. The knowledge of particular properties of α-L-LNA TFOs can provide insights that are useful for further progress in rational design of molecules capable of specifically recognizing the dsDNA helix.

To improve the binding properties of LNA TFOs at higher pH, we additionally introduce herein a new LNA nucleoside containing N^7-glycosylated guanine as a nucleobase. It has been shown that N^7-deoxyguanosine (d^7G) mimics protonated cytosine and specifically binds GC base pairs within a parallel triple helix motif.[28] The stabilities of d^7G-containing triplexes are independent of pH but strongly dependent on the sequence context. The TFOs containing d^7G are particularly useful for targeting continuous GC base pairs.[29]

2. Results and discussion

The first synthesis of α-L-LNA 3′-*O*-phosphoramidites containing thymine, 5-methylcytosine, and adenine nucleobases was reported by Wengel.[25,26] However, to make α-L-LNA practically available, a significantly improved and more efficient route to α-L-LNA monomers has been developed (Scheme 1). Analogous to commercially available LNA

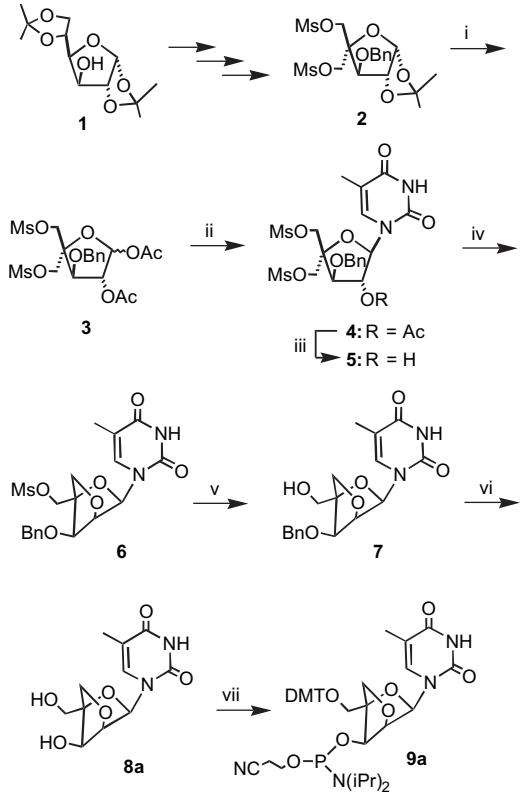

Scheme 1. *Reagents and conditions*: (i) Ac_2O, concd H_2SO_4, AcOH, 91%; (ii) thymine, BSA, trimethylsilyl triflate, MeCN, quant.; (iii) HCl, MeOH, 99%; (iv) (a) MsCl, pyridine; (b) NaOH, H_2O, quant.; (v) (a) NaOBz, DMSO; (b) NaOH, H_2O, 74%; (vi) 20% $Pd(OH)_2$/C, HCO_2NH_4, MeOH, 1,4-dioxane, reflux, 93%; (vii) (a) DMT-Cl, pyridine; (b) 2-cyanoethyl-*N*,*N*,*N*′,*N*′ -tetraisopropylphosphordiamidite, 4,5-dicyanoimidazole, CH_2Cl_2, 92%, Ref. 31.

nucleosides,[24] a convergent strategy was chosen for the production of α-L-LNA. A starting material for the synthesis of α-L-LNA-T phosphoramidite **9a** (Scheme 1), the known 4-C-branched furanose **2**,[25] was obtained from commercial 1,2:5,6-di-*O*-isopropylidene-α-D-glucofuranose **1** as described earlier. However, NMR data reported by Wengel[25] for compound **2** was significantly different from that reported here. Coupling sugar **3** was subsequently obtained in 91% yield after one-pot acetolysis and acetylation of **2**. The anomeric mixture **3** was then used as a glycosyl donor for Vorbrügen-type[30] coupling reaction with silylated thymine to give a 4′-C-branched nucleoside **4** after standard aqueous work-up. Transformation of compound **4** into α-L-*ribo*-configured LNA-T derivative **6** required epimerization at the 2′-position. To make this inversion, the 2′-*O*-acetyl group was first replaced with mesyl and the resulting compound was then treated with aqueous sodium hydroxide. Accordingly, treatment of **4** with methanolic hydrochloride resulted in quantitative removal of the acetyl group to give intermediate **5**. In the same flask, the solvents were replaced by anhydrous pyridine and **5** was consecutively treated with mesyl chloride and sodium hydroxide to give protected α-L-LNA-T nucleoside **6**. Apparently, the transformation of **5** into **6** proceeded via the 2,2′-anhydro intermediate, which could be consecutively formed, hydrolyzed, and subjected to ring-closure reaction in the same reaction mixture.[26] Indeed, corresponding intermediates were detected by RP-HPLC analyses of the reaction mixture (data not shown). This reaction cascade proceeded very smoothly and was completed overnight in nearly quantitative yield. The purity of nucleoside **6** was about 96% (RP-HPLC, integration at 260 nm) after aqueous work-up and the compound was used further without additional purification. Instead, **6** was converted to crystalline compound **7** after deprotection of the 5′-hydroxy group. Thus, nucleoside **6** was reacted with sodium benzoate in hot DMSO and the obtained 5′-benzoate was hydrolyzed by the excess of alkali to give **7** in 67% yield (from **2**) after crystallization from ethyl acetate. As expected, catalytic removal of the 3′-*O*-benzyl group from **7** easily afforded diol **8a** in 93% yield after crystallization from water. Finally, α-L-LNA-T phosphoramidite building block **9a** was derived from **8a** by means of the standard methods.[26,31] The synthetic route to phosphoramidite **9a** described above is significantly superior to the earlier reported procedure,[25,26] which makes the commercial production of α-L-LNA-T nucleoside very feasible.

An important limitation of the triplex technology is that parallel triplexes require conditions of low pH, which are necessary for protonation of the nitrogen at position 3 of cytosines in TFOs (Fig. 2). To address this problem, several derivations of cytosine analogues have been introduced that provide less pH-dependent triplex formation. Thus, 5-methylcytosine (mC) replacement for cytosine in the DNA TFOs gave more stable triplexes at neutral pH, because of the increase in pK_a for 5-methylcytosine (4.3) compared with cytosine (4.15).[32] A similar effect has recently been demonstrated for LNA and ENA modified TFOs.[22,33] For this reason, we concentrated on studying α-L-LNA-modified TFOs containing thymine and 5-methylcytosine nucleobases.

It has already been reported[25,34] that both α-L-LNA-mC and LNA-mC phosphoramidites **13a**,**b** (Scheme 2) could be

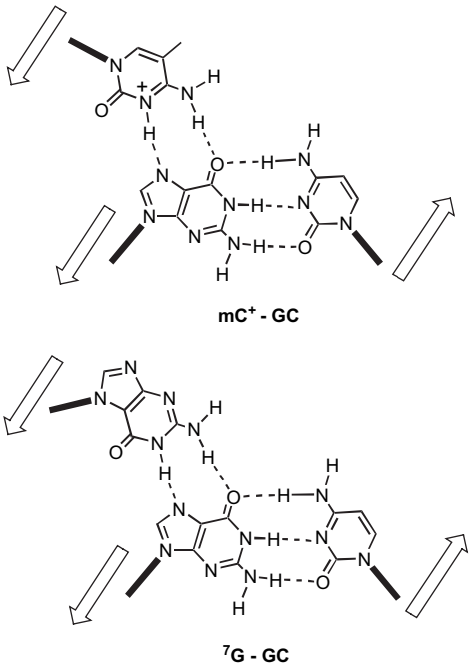

Figure 2. Schematic comparison of the base triplets involving 5-methylcytosine (mC) and N^7-glycosylated guanine (^{7}G).[28,29]

derived by different methods from the corresponding thymin-1-yl diols **8a**,**b**. The recent developments for a universal (both for LNA and α-L-LNA) scale-up synthesis of **13a**,**b** are depicted in Scheme 2. The method has several advanced points, which make it considerably more useful in comparison to already reported procedures. Thus, starting with α-L-LNA-T diol **8a**, fully carbohydride protected thymin-1-yl derivative **10a** was easily produced after one-pot consecutive treatment of **8a** with DMT-chloride and acetic anhydride in anhydrous pyridine. The introduction of a hydrophobic DMT group at this stage significantly facilitated handling of nucleosides in later steps of the synthesis. The 3′-*O*-acetyl

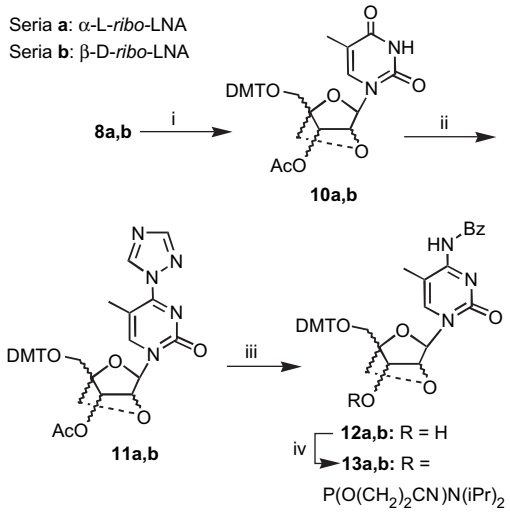

Scheme 2. *Reagents and conditions*: (i) (a) DMT-Cl, pyridine; (b) Ac_2O, pyridine, 90% (**10a**) and 89% (**10b**); (ii) 1,2,4-triazole, $POCl_3$, DIPEA, MeCN, 97% (**11a**) and 90% (**11b**); (iii) (a) concd NH_4OH, MeCN; (b) Bz_2O, pyridine; (c) NaOH, pyridine, MeOH, H_2O, 81% (**12a**) and 76% (**12b**); (iv) 2-cyanoethyl-*N*,*N*,*N*′,*N*′-tetraisopropylphosphordiamidite, 4,5-dicyanoimidazole, CH_2Cl_2, 95%, Ref. 31.

protection group was selected due to the simplicity of its introduction and removal, avoiding undesired side reactions. Second, nucleoside **10a** was almost quantitatively converted to a stable 4-(1,2,4-triazol-1-yl) derivative **11a** by the method of Reese.[35] Accordingly, **10a** was treated with freshly distilled phosphoryl chloride in the presence of 1,2,4-triazole and excess of a base to give **11a** after aqueous work-up. Compound **11a** can serve as a valuable intermediate in the synthesis of different 4-substituted α-L-LNA-pyrimidine nucleosides as it can be easily handled and stored. Thus, a simple procedure was applied to convert **11a** to 4-*N*-benzoyl-cytosine-1-yl derivative **12a** (Scheme 2). After compound **11a** was allowed to react with ammonia overnight, the solvents were thoroughly removed and the residue was treated with benzoic anhydride in anhydrous pyridine to give a mixture of mono- and di-benzoylated (MALDI-MS analysis) nucleosides. Addition of aqueous sodium hydroxide to the same reaction mixture led to very selective hydrolysis of undesired 3′-benzoate leaving the intact nucleoside **12a**. The nucleoside **12a** was isolated in 81% yield by column chromatography and phosphitylated using the method used for the production of **9a**.[31] The above synthetic procedures were also successfully applied for the preparation of phosphoramidite **13b** (Scheme 2), which established them as a reliable universal method for the production of both LNA and α-L-LNA monomers **13a**,**b**.

The unnatural N^7-glycosylated deoxyguanosine was introduced as another promising replacement for cytosine in TFOs[28] (Fig. 2). To investigate compatibility of this approach with LNA technology, TFOs modified with LNA-^{7}G were synthesized. The synthesis of phosphoramidite monomers **20** and **23** was first attempted (Scheme 3). The coupling of silylated 2-*N*-isobutyrylguanine with glycosyl donor **14** was already reported.[24] In the reaction conditions (trimethylsilyl triflate as a catalyst in 1,2-dichloromethane; reflux), N^7-glycosylated compound **15** was formed as a minor product in approximately 10% yield along with N^9-isomeric counterpart. However, when conditions favoring the formation of N^7-isomer[28,29] were applied, **15** was produced as the sole product after chromatographic purification albeit in moderate 34% yield (Scheme 3). The correct structure of the obtained isomer was confirmed by comparison of NMR data for **15** with that published for N^7- and N^9-glycosylated guanines.[36,37] Thus, the most characteristic signal corresponding to C5 positioned at 110.2 ppm in the ^{13}C NMR spectrum of **15**. The conversion of nucleoside **15** to diol **19** was performed generally following the synthetic route developed for N^9-glycosylated LNA-G.[24] Accordingly, the ring-closure reaction promoted in **15** by sodium hydroxide afforded protected LNA-^{7}G nucleoside **16**. The 5′-methylsulfonate of **16** was displaced by benzoate to give **17**, which in turn was hydrolyzed to furnish nucleoside **18**. To keep 2-*N*-isobutyryl intact, debenzylation of **18** was carried out on Pd/C using formic acid as a hydrogen supply[24] to give diol **19**. Monomeric unit **20**, finally derived from **19**, was successfully applied for automated oligonucleotide synthesis using the phosphoramidite method.[38] However, the 2-*N*-isobutyryl group of the LNA-^{7}G mononucleotide turned out to be considerably more stable in comparison to all the other commonly used protections. Therefore, modifications of deprotection procedure were required for LNA-^{7}G containing oligonucleotide after the synthesis (vide infra). To facilitate the synthesis of oligonucleotides containing multiple LNA-^{7}G modifications, (dimethylamino)methylidene[39] protected phosphoramidite **23** was ultimately produced. Thus, the fully deprotected nucleoside **21** was furnished in 86% yield after consecutive catalytic hydrogenation and treatment with ammonium hydroxide of **18**. 2-*N*-(Dimethylamino)methylidene and 5′-*O*-DMT groups were introduced into **21** by conventional

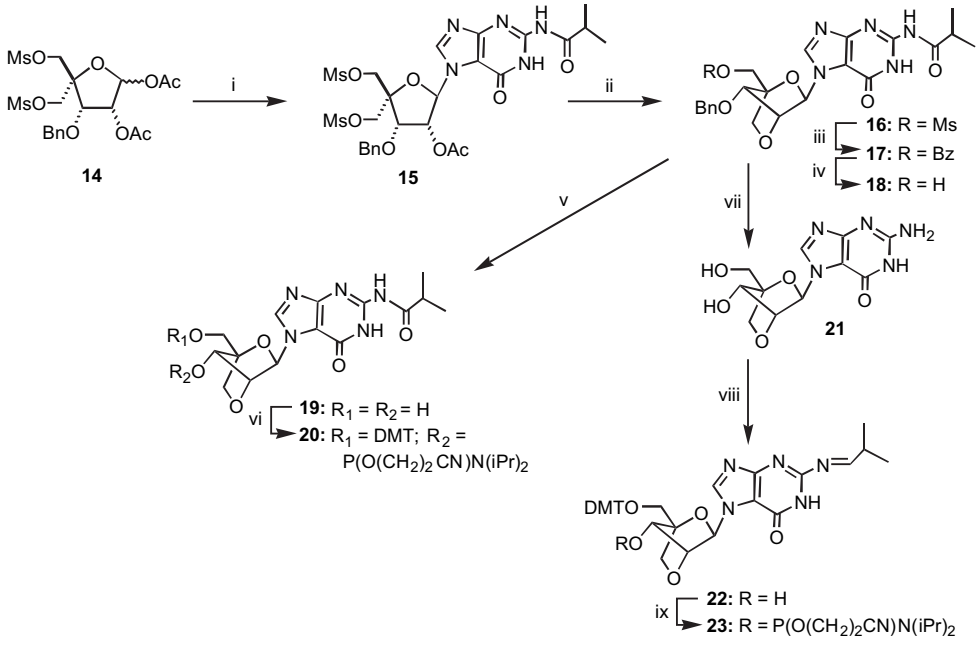

Scheme 3. *Reagents and conditions*: (i) 2-*N*-isobutyrylguanine, BSA, $SnCl_4$, MeCN, 34%; (ii) NaOH,1,4-dioxane, H_2O, 89%; (iii) NaOBz, DMF, 93%; (iv) NaOH, pyridine, EtOH, H_2O, 85%; (v) 10% Pd/C, HCO_2H, MeOH, 81%; (vi) (a) DMT-Cl, pyridine; (b) 2-cyanoethyl-*N*,*N*,*N*′,*N*′-tetraisopropylphosphordiamidite, 4,5-dicyanoimidazole, CH_2Cl_2, 82%; (vii) (a) 10 % Pd/C, HCO_2NH_4, MeOH; (b) NH_3, MeOH, 86%; (viii) (a) *N*,*N*-dimethylformamide dimethyl acetal, DMF; (b) DMT-Cl, pyridine, 89%; (ix) 2-cyanoethyl-*N*,*N*,*N*′,*N*′-tetraisopropylphosphordiamidite, 4,5-dicyanoimidazole, CH_2Cl_2, MeCN, 92%.

methods[36] and compound **22** was isolated in 89% yield after column chromatography. Phosphoramidite **23** was derived from **22** in 92% yield generally following the procedure developed for other LNA nucleosides.[31]

Along with commercially available DNA and LNA phosphoramidites, the phosphoramidite building blocks **9a**, **13a**, and **23** were used for automated oligonucleotide synthesis to produce the LNA oligonucleotides depicted in Tables 1 and 2. The standard protocols of DNA synthesis were applied for all LNA and α-L-LNA amidites, except for coupling (extended to 500 s) and oxidation cycles (extended to 30 s). After synthesis, the oligonucleotides were deprotected by treatment with concentrated ammonium hydroxide for 6 h at 60 °C and purified by RP-HPLC. To synthesize LNA-^{7}G modified oligonucleotide **46** (Table 2), phosphoramidite **20** was used instead of **23**. The above conditions for the automated synthesis were also successfully applied in this case. However, the deprotection procedure was modified in order to complete the removal of the 2-*N*-isobutyryl group from LNA-^{7}G mononucleotide. Thus, ammonium hydroxide treatment used during the synthesis of all the other oligonucleotides was first applied. MALDI-MS analysis of the mixture, however, revealed the presence of a product (a signal of approximately equal intensity as for the target product) containing intact isobutyryl protection group. This signal completely disappeared after additional treatment of the reaction mixture with aqueous methylamine for 2 h at 60 °C. Analogous data demonstrating the increased stability of the 2-*N*-isobutyryl group on N^7-glycosylated guanine have been previously reported by Dervan.[29]

Triplex-forming properties of α-L-LNA-modified oligonucleotides were assessed against target DNA duplex containing an oligopurine–oligopyrimidine sequence of 14 bp in the central core and presented in Table 1 as melting temperatures of the corresponding triplexes. The recently reported results on binding properties of LNA and ENA TFOs[22,33] have been obtained by studying the same oligonucleotide model and can be directly compared with the data reported herein. Thus, in good agreement with the data reported by Imanishi,[33] the sequences of alternating LNA and DNA nucleotides **24** and **25** (Table 1, entries 1 and 2) formed stable triplexes with the complementary duplex **40**·**41** in the pH range 6.5–7.5. It was found that stability of triplex **25**:**40**·**41** slightly exceeds stability of **24**:**40**·**41** at pH 6.5. This observation clearly parallels the rules derived recently for designing LNA-modified TFOs.[40] Accordingly, the sequence effect and the differential stabilization by LNA-T and LNA-mC nucleotides have been pointed out.[40] For LNA-modified TFOs, maximizing the number of LNA5′–3′DNA steps (e.g., by the use of an LNA nucleotide

Table 1. Melting temperatures[a] of the perfectly matched triplexes (±1 °C) and duplexes (±0.5 °C) containing β-D- and α-L-LNA nucleotides

Entry	Oligo structure (5′–3′) (compound number)	Parallel triplex[b] at diff. pH			Antiparallel duplex[c]
		pH 6.5	pH 7.0	pH 7.5	
1	tCtCtCtCcCtTtT (**24**)	56.5	43.0	32.0	71.8
2	TcTcTcTcCcTtTt (**25**)	58.5	41.5	27.5	71.7
3	t*X*t*X*t*X*c*X*t*Y*t*Y* (**26**)	45.0	30.5	nt[d]	68.4
4	*YXYXYXYXXXYYYY* (**27**)	36.0	25.5	nt	90.5
5	*YCYCYCYCXCYTYT* (**28**)	20.0	nt	nt	83.4
6	tCtCtCt*X*cCtTtT (**29**)	57.5	43.0	31.5	70.6
7	TcTcTc*Y*cCcTtTt (**30**)	47.0	29.0	nt	68.4
8	Tc*Y*cTc*Y*cCc*Y*tTt (**31**)	37.0	21.0	nt	66.5
9	tCt*X*tCt*X*cCt*Y*tT (**32**)	52.0	38.0	27.0	69.3
10	t^{7}Gt^{7}Gt^{7}Gt^{7}Gc^{7}GtTtT (**33**)	nt	nt	nt	nt
11	t^{7}GtCt^{7}GtCc^{7}GtTtT (**34**)	nt	nt	nt	45.7
12	t^{7}GtCt^{7}Gtc^{7}GctTtT (**35**)	41.5	34.0	nt	41.5
13	t^{7}Gtct^{7}Gtc^{7}GcttTt (**36**)	38.0	28.0	nt	36.6
14	tCtCtCt^{7}GcCtTtT (**37**)	57.0	44.5	34.5	59.6
15	TcTcTcTc^{7}GcTtTt (**38**)	>60	45.5	31.0	59.5
16	Tc*Y*cTc*Y*c^{7}Gc*Y*tTt (**39**)	41.5	27.5	nt	56.5

[a] The melting temperatures (T_m values) were obtained as maxima of the first derivatives of the corresponding melting curves (optical density at 260 nm versus temperature). Presented as the mean of three measurements. LNA residues are capitalized. ^{7}G=β-D-LNA-G (N^7-isomer); *X*=α-L-LNA-mC; *Y*=α-L-LNA-T. C, c=5-methyl-cytosines.

[b] The model complementary duplex (1 μM) was obtained by mixing purine strand **40**: 5′-gaacaaacagagagagggaaaatcccccta and pyrimidine strand **41**: 5′-tagggggattttccctctctctgtttgttc in 0.01 M Na-phosphate buffer (pH 6.5, 7.0, or 7.5) containing 0.1 M NaCl and 1 mM EDTA. Concentration of TFOs: 1 μM.

[c] T_ms of the antiparallel duplexes were measured against complementary tetradecadeoxynucleotide **42**: 5′-aaaagggagagaga. Concentration of duplexes: 1 μM; the same buffer as for triplex study (pH 7.4).

[d] nt—No cooperative transition observed over 20 °C.

Table 2. Melting temperatures (±1 °C) of the perfectly matched and singly mismatched LNA·DNA duplexes[a]

Entry	Oligonucleotide structure (5′–3′)	T_ms (±1 °C) of the duplexes with complementary deoxynucleotides			
		3′-ctg*a*atcc (**47**)	3′-ctg*t*atcc (**48**)	3′-ctg*g*atcc (**49**)	3′-ctg*c*atcc (**50**)
1	GAC*T*TAGG (**43**)	**61**	28	36	24
2	GAC*A*TAGG (**44**)	38	**62**	43	41
3	GAC*G*TAGG (**45**)	32	55	41	**71**
4	GAC^7*G*TAGG (**46**)	nt	32	37	31

[a] Concentration of duplexes: 2.5 μM. All other experimental conditions and abbreviations as in Table 1.

at 5′-end as for **25**) and maximizing the use of LNA-T is thermodynamically preferable for triplex formation. On the other hand, it has been reported[41] that triplex formation in the pyrimidine motif proceeds from the 5′-end to the 3′-end according to the nucleation–zipping mechanism. Association rate is thus governed by the composition of base triplets on the 5′-end of the triplex, which are significantly different for **24** and **25**. According to this model, oligonucleotide **25** containing two LNA-T nucleotides at the 5′-end might presumably bind to duplex **40**·**41** slightly faster than its counterpart **24**.

The thermostability of triplex **24**:**40**·**41**, however, demonstrated a notably lower pH dependence than stability of **25**:**40**·**41** (Table 1, entries 1 and 2). The higher apparent pK_a of the LNA-modified 5-methylcytidines in the dsDNA:LNA triplex has been attributed to lowered base-pair dissociation rates.[23] Therefore, due to the increased number of LNA-mC nucleotides in **24** compared with isosequential **25**, the stability of triplex **24**:**40**·**41** at pH 7.5 is already 4.5 °C higher.

The triplex-forming ability of α-L-LNA-modified TFOs turned out to be significantly reduced in comparison to LNA TFOs. Thus, replacement of LNA nucleotides in **24** by analogous α-L-LNA monomers resulted in a T_m decrease of the corresponding triplex by 11.5 °C at pH 6.5 (triplex **26**:**40**·**41**; entry 3). The fully modified α-L-LNA oligonucleotide **27** (Table 1, entry 4) was able to bind the complementary DNA duplex **40**·**41** at pH 6.5 and 7.0, albeit with reduced affinity. These data are particularly interesting, considering the fact that no stable triplexes have been detected for fully modified LNA TFOs.[33]

The attempt to construct a potent TFO consisting of altering LNA and α-L-LNA units failed as oligonucleotide **28** (Table 1, entry 5) did not form a stable triplex with **40**·**41**. However, LNA TFO **24** could tolerate a single α-L-LNA replacement for LNA-mC monomer. Thus, a DNA/LNA/α-L-LNA chimera **29** demonstrated the same binding properties as the parent **24** (compare entries 1 and 6). In sharp contrast to **29**, a single α-L-LNA-T replacement made for LNA-T in **25** resulted in significant destabilization of the triplex demonstrating differential pairing abilities of α-L-LNA-T and α-L-LNA-mC units in TFOs. This phenomenon was additionally confirmed by triple α-L-LNA-T replacements for LNA-T. The T_m value for the triplex formed by chimera **31** (entry 8) containing three α-L-LNA-T units is already 21.5 °C lower than T_m of **25**:**40**·**41**. At the same time, oligonucleotide **32** containing two α-L-LNA-mC and only a single α-L-LNA-T modification bound to the model duplex with significantly higher potency (compare entries 8 and 9; Table 1).

Binding properties of TFOs modified with LNA-^{7}G are presented in entries 10–16 (Table 1). Thus, TFOs **33** and **34** containing five or three LNA-^{7}G residues instead of LNA-mC did not bind to **40**·**41** at any pH. However, a further experiment demonstrated that DNA/LNA chimeras modified with three LNA-^{7}G could form triplexes when LNA-^{7}G units were separated by two DNA mononucleotides (TFOs **35** and **36**; entries 12 and 13). Importantly, the improved pH dependence observed for triplex stability in this case indicates that LNA-^{7}G units were involved in triplex formation by pairing mode as suggested by Dervan[28,29] (Fig. 2). The most stable triplexes were detected for TFOs **37** and **38** (entries 14 and 15) containing a single LNA-^{7}G replacement for LNA-mC (entries 14 and 15). Accordingly, at pH 6.5, **37** bound to the model duplex with the same efficacy as parent **24**. However, the melting temperature of **37**:**40**·**41** was detectably higher than T_m of **24**:**40**·**41** at pH 7.5 (compare entries 1 and 14). The melting temperature of the triplex formed by **38** (entry 15) at pH 6.5 was close to T_m of duplex **40**·**41** and could not be measured by the used method. Nevertheless, remarkable T_ms=45.5 and 31.0 °C were measured for **38**:**40**·**41** at pH 7.0 and 7.5, respectively. Noteworthy, a lower pH sensitivity of T_m for triplex formed by **37** in comparison to **38** (Table 1, entries 14 and 15) can be explained by the higher content of LNA-mC nucleotides as was already pointed out for TFOs **24** and **25** (vide supra). The stabilizing effect of the single LNA-^{7}G modification was also shown in the case of DNA/LNA/α-L-LNA chimera **39** (compare entries 8 and 16).

Binding properties of LNA-^{7}G were further studied in the antiparallel duplex context. It was shown that single LNA-^{7}G replacement for the internal LNA-mC nucleotide resulted in significant destabilization (by 10–12 °C) of the antiparallel duplex with complementary oligodeoxynucleotide **42** (Table 1, entries 14–16). Furthermore, an additive destabilizing effect of multiple LNA-^{7}G modifications was shown for the complementary duplexes involving DNA/LNA chimerical oligonucleotides **33**–**36** (entries 10–13). Incompatibility of LNA-^{7}G with Watson–Crick duplex geometry was also demonstrated for a fully modified LNA oligonucleotide of random sequence. When incorporated into LNA octanucleotide **46**, LNA-^{7}G was unable to efficiently pair with any natural DNA base (Table 2, entry 4). The melting temperatures measured for duplexes formed by **46** against **47**–**50** were very low, close to the T_ms of the most unstable mismatched duplexes formed by unmodified **43**–**45** (entries 1–3). Thus, replacement of LNA-G with unnatural LNA-^{7}G led to destabilization of the complementary duplex against **50** by 40 °C (compare duplexes **45**·**50** and **46**·**50**). The discriminating pairing properties of the single LNA-^{7}G modification can be very useful for in vivo application of alternating DNA/LNA TFOs in order to minimize undesired competitive biding to nucleic acids in the antiparallel duplex mode.

3. Conclusions

In conclusion, we developed an improved method for scaled-up synthesis of the building blocks for oligonucleotides containing α-L-LNA thymine and 5-methylcytosine units as well as a method for synthesis of the novel N^7-glycosylated LNA-guanosine monomer. The compounds were successfully incorporated into triplex-forming oligonucleotides and their binding properties were systematically studied. Pyrimidine DNA/α-L-LNA chimeras demonstrate a reduced binding ability compared with the analogous DNA/LNA TFOs. However, in contrast to LNA TFOs, the fully modified α-L-LNA form a stable triplex with the model DNA duplex. The alternating DNA/LNA TFOs containing a single LNA-^{7}G replacement for internal LNA-mC demonstrate improved pH-dependent properties and can also be used to discriminatively reduce competitive binding of TFOs to

nucleic acids in the antiparallel duplex mode. Our findings may be useful for further developments in the field of triplex technology.

4. Experimental

4.1. General

All chemicals were obtained from commercial suppliers and were used without additional purification. An atmosphere of nitrogen was applied when reactions were conducted in anhydrous solvents. Column chromatography was performed using Silica gel 60 (0.063–0.200 mm) from Merck and HPLC using a column Prep Nova-Pak HR Silica 60 (6 μm, 30×300 mm). Analytical reverse-phase chromatography (RP-HPLC) was performed on XTerra RP_{18} 5 μm (3.9×150 mm) column using Delivery System and Dual λ Absorbance Detector (all from Waters) in the following eluent system: linear gradient 20–100% v/v of MeCN in 0.05 M aqueous triethylammonium acetate (pH 7.2) during 15 min. Flow rate: 1 mL/min. R_t—retention time. $A_{290/260}$—the ratio between absorbance at 290 and 260 mn measured at maximum of the corresponding peak. All ^{1}H and ^{31}P NMR spectra were recorded at 400 and 161.9 MHz, respectively. ^{13}C NMR spectra for **10a**, **10b**, **16**, and **18** were recorded at 62.9 MHz and at 100.6 MHz for all other compounds. The values for chemical shifts are reported in parts per million relative to tetramethylsilane (TMS) as internal standard for ^{1}H and ^{13}C, and relative to 85% H_3PO_4 as external standard for ^{31}P. MALDI-TOF mass spectra of nucleosides were recorded on a Voyager-DE PRO spectrometer in positive ion mode using 2,5-dihydroxybenzoic acid as the matrix. Melting points were measured on a Büchi Melting Point B-540 apparatus and uncorrected. The mp values are reported for all crystalline compounds. All the other solid products were obtained as amorphous solid foam after chromatographic purification and generally demonstrated broad phase transitions.

4.1.1. 3-*O*-Benzyl-4-*C*-methanesulfonoxymethyl-5-*O*-methanesulfonyl-1,2-*O*-isopropylidene-β-L-*threo*-pentofuranose (2). Colorless viscous oil; obtained as described earlier.[25] ^{1}H NMR ($CDCl_3$): δ 7.40–7.31 (m, 5H), 5.98 (d, *J*=4.0 Hz, 1H), 4.71 (d, *J*=11.5 Hz, 1H), 4.70 (d, *J*=3.9 Hz, 1H), 4.55 (d, *J*=11.5 Hz, 1H), 4.39 (d, *J*=10.4 Hz, 1H), 4.38 (d, *J*=10.8 Hz, 1H), 4.33 (d, *J*=10.6 Hz, 2H), 4.10 (s, 1H), 3.02 (s, 3H), 3.00 (s, 3H), 1.57 (s, 3H), 1.33 (s, 3H). ^{13}C NMR ($CDCl_3$) δ 136.1, 128.5, 128.3, 127.9, 113.2, 105.7, 85.9, 84.0, 82.8, 72.7, 67.3, 67.0, 37.5, 37.3, 26.4, 25.8. MALDI-TOF MS: *m*/*z* 489.0 ($M+Na^+$).

4.1.2. 1,2-Di-*O*-acetyl-3-*O*-benzyl-4-*C*-methanesulfonoxymethyl-5-*O*-methanesulfonyl-α,β-L-*threo*-pentofuranose (3). To a solution of furanose **2** (73.4 g, 0.157 mol) in AcOH (250 mL) were added Ac_2O (40 mL, 0.424 mol) and concd H_2SO_4 (1.1 mL). The solution was stirred overnight, cooled in an ice bath, and 2 M NaOH (400 mL) was added under intensive stirring. The mixture was washed with CH_2Cl_2 (3×200 mL). The combined organic layers were washed with saturated $NaHCO_3$ (2×400 mL) and brine (400 mL), dried (Na_2SO_4), and concentrated under reduced pressure to give **3** (72.6 g, 91%) as a brownish viscous oil.[25]

4.1.3. 1-(2-*O*-Acetyl-3-*O*-benzyl-4-*C*-methanesulfonoxymethyl-5-*O*-methanesulfonyl-α-L-*threo*-pentofuranosyl)thymine (4). A mixture of furanose **3** (72.4 g, 0.14 mol) and thymine (22.5 g, 0.18 mol) was suspended in anhydrous MeCN (300 mL) and *N*,*O*-bis(trimethylsilyl)acetamide (68 mL, 0.27 mol) was added. After refluxing for 1.5 h, a clear solution was obtained and the mixture was cooled to room temperature. Trimethylsilyl trifluoromethanesulfonate (50 mL, 0.28 mol) was added and refluxing was continued for 6 h. The reaction mixture was cooled to room temperature, neutralized with saturated $NaHCO_3$ (400 mL), and washed with CH_2Cl_2 (2×300 mL). The combined organic layers were washed with saturated $NaHCO_3$ (2×300 mL), dried (Na_2SO_4), and concentrated under reduced pressure to give compound **4** (84.0 g, 103%) as a brownish solid residue, which was used for the next step without additional purification. RP-HPLC: R_t=9.85 min, $A_{290/260}$=0.12, purity 97% (integration at 260 nm). Analytical sample was obtained after silica gel column chromatography (1–3% v/v MeOH/CH_2Cl_2) as a white solid foam. ^{1}H NMR ($CDCl_3$): δ 9.34 (br s, 1H), 7.31–7.42 (m, 6H), 6.28 (d, *J*=3.5 Hz, 1H), 5.36 (dd, *J*=3.5 and 2.8 Hz, 1H), 4.78 (d, *J*=11.4 Hz, 1H), 4.66 (d, *J*=11.4 Hz, 1H), 4.55 (d, *J*=11.2 Hz, 1H), 4.42 (d, *J*=11.2 Hz, 1H), 4.35 (d, *J*=10.8 Hz, 1H), 4.26 (d, *J*=10.8 Hz, 1H), 4.25 (d, *J*=2.8 Hz, 1H), 3.05 (s, 3H), 3.02 (s, 3H), 2.14 (s, 3H), 1.80 (d, *J*=1.1 Hz, 3H). ^{13}C NMR ($CDCl_3$): δ 169.6, 163.3, 150.3, 135.8, 134.9, 128.6, 128.5, 128.3, 112.3, 87.5, 84.6, 81.1, 79.3, 73.0, 66.9, 65.4, 37.6, 20.5, 12.2. MALDI-TOF MS: *m*/*z* 599.1 ($M+Na^+$). Anal. Calcd for $C_{22}H_{28}N_2O_{12}S_2$: C, 45.83; H, 4.89; N, 4.86. Found: C, 45.97; H, 4.86; N, 4.80.

4.1.4. 1-(3-*O*-Benzyl-5-*O*-methanesulfonyl-2-*O*,4-*C*-methylene-α-L-ribofuranosyl)thymine (6). Compound **4** (83.7 g, 0.145 mol) was dissolved in 1 M HCl in MeOH (450 mL) and stirred for 24 h. The solvents were removed under reduced pressure to give a solid residue. The residue was co-evaporated with anhydrous MeCN (250 mL) and dried in vacuo overnight to give intermediate **5** (77.2 g, 99.6 %). RP-HPLC: R_t=8.82 min, $A_{290/260}$=0.155. The intermediate was dissolved in anhydrous pyridine (200 mL), cooled in an ice bath, and MsCl (14.5 mL, 0.183 mol) was added under intensive stirring. The mixture was allowed to warm to room temperature and stirred overnight, whereupon 1 M NaOH (1.5 L) was added. After stirring for 18 h, AcOH (90 mL) was added and the mixture was washed with CH_2Cl_2 (2×400 mL). The combined organic layers were washed with saturated $NaHCO_3$, dried (Na_2SO_4), and concentrated under reduced pressure to give an oily residue. The residue was co-evaporated with anhydrous toluene (2×300 mL) and dried in vacuo to give compound **6** (64.8 g, 102%) as a brown solid material. RP-HPLC: R_t=8.75 min, $A_{290/260}$=0.28, purity 96% (integration at 260 nm). Analytical sample was obtained after silica gel column chromatography (1.5–3.5% v/v MeOH/CH_2Cl_2) as a white solid foam. ^{1}H NMR (DMSO-d_6): δ 11.40 (br s, 1H), 7.64 (d, J=1.1 Hz, 1H), 7.40–7.30 (m, 5H), 5.96 (s, 1H), 4.71 (d, *J*=12.1 Hz, 1H), 4.68 (d, *J*=12.1 Hz, 1H), 4.60 (m, 3H), 4.50 (s, 1H), 4.12 (d, *J*=8.6 Hz, 1H), 4.00 (d, *J*=8.5 Hz, 1H), 3.25 (s, 3H), 1.84 (d, *J*=1.1 Hz, 3H). ^{13}C NMR (DMSO-d_6): δ 163.8, 150.3, 137.7, 135.8, 128.4, 127.8, 127.6, 108.3, 86.8, 86.5, 79.2, 76.5, 72.0, 71.3, 65.3, 37.0, 12.3. MALDI-TOF MS: *m*/*z* 460.8 ($M+Na^+$).

4.1.5. 1-(3-*O*-Benzyl-2-*O*,4-*C*-methylene-α-L-ribofuranosyl)thymine (7). A mixture of **6** (64.0 g, 0.146 mol) and NaOBz (41 g, 0.285 mol) suspended in anhydrous DMSO (450 mL) was stirred for 3 h at 120 °C. The mixture was cooled to room temperature and 1 M NaOH (500 mL) was added under intensive stirring. The obtained clear solution was stirred for 1 h, neutralized with AcOH (30 mL), and washed with CH_2Cl_2 (3×300 mL). The combined organic layers were filtered through a silica gel pad (300 cm^3); silica gel was washed with 4% MeOH/CH_2Cl_2 (v/v, 500 mL). The combined filtrates were dried (Na_2SO_4) and concentrated under reduced pressure at 70 °C until complete removal of DMSO. The solid residue was crystallized from EtOAc to give nucleoside **7** (30.5 g) as a white powder. The mother liquor was concentrated to a solid residue and applied to silica gel column chromatography (1–4% v/v MeOH/CH_2Cl_2). The fractions containing **7** were pooled, concentrated under reduced pressure, and the residue was crystallized from EtOAc to give another 8.4 g of **7** (total yield 74%). Mp 169–170 °C. MALDI-TOF MS: *m/z* 382.7 ($M+Na^+$). Anal. Calcd for $C_{18}H_{20}N_2O_6$: C, 55.99; H, 5.59; N, 7.77. Found: C, 60.02; H, 5.47; N, 7.79. NMR data were identical with those reported earlier.[26]

4.1.6. 1-(2-*O*,4-*C*-Methylene-α-L-ribofuranosyl)thymine (8a). To a solution of compound **7** (30.4 g, 84 mmol) in MeOH/1,4-dioxane (1:1 v/v, 200 mL) were added $Pd(OH)_2$/C (6 g) and HCO_2NH_4 (15 g). The mixture was stirred under reflux for 1 h. More HCO_2NH_4 was added in portions of 5 g at an interval of 30 min (total amount 25 g). The mixture was cooled to room temperature, diluted with 30% aqueous NH_4OH (50 mL), and filtered through a Celite pad. The Celite was washed with 30% aqueous NH_4OH (75 mL). The filtrates were combined, concentrated under reduced pressure to ca. half of its volume and kept at 4 °C overnight. The precipitate formed was collected by filtration, washed with cold H_2O, and dried in vacuo to give compound **8a** (21.1 g, 93%) as a white crystalline powder. Mp 239–242 °C (dec.); starts sintering at 234 °C. MALDI-TOF MS: *m/z* 292.9 ($M+Na^+$). Anal. Calcd for $C_{11}H_{14}N_2O_6 \cdot 1/5H_2O$: C, 48.25; H, 5.30; N, 10.23. Found: C, 48.18; H, 5.16; N, 10.23. NMR data were identical with those reported earlier.[26]

4.1.7. 1-[3-*O*-Acetyl-5-*O*-(4,4′-dimethoxytrityl)-2-*O*,4-*C*-methylene-α-L-ribofuranosyl]thymine (10a). To a solution of compound **8a** (9.13 g, 33.8 mmol) in anhydrous pyridine (60 mL) was added DMT-Cl (14.2 g, 42.2 mmol). The mixture was stirred for 4 h and Ac_2O (4.5 mL, 43.9 mmol) was added. After stirring overnight, the mixture was diluted with EtOAc (250 mL), washed with saturated $NaHCO_3$ (2×300 mL), dried (Na_2SO_4), and concentrated under reduced pressure to an oily residue. The residue was co-evaporated with toluene (2×200 mL) and purified by silica gel column chromatography (0.5–2% v/v MeOH/CH_2Cl_2, containing 1% of Et_3N) to give compound **10a** (18.7 g, 90%) as a white solid foam. ^1H NMR (DMSO-d_6): δ 11.46 (br s, 1H), 7.62 (d, *J*=1.1 Hz, 1H), 7.41–7.24 (m, 9H), 6.91 (m, 4H), 6.12 (s, 1H), 5.45 (s, 1H), 4.55 (s, 1H), 4.18 (d, *J*=8.8 Hz, 1H), 3.86 (d, *J*=8.8 Hz, 1H), 3.74 (s, 6H), 3.32 (m, 2H; overlaps with H_2O), 2.04 (s, 3H), 1.84 (d, *J*=1.1 Hz, 3H). ^{13}C NMR (DMSO-d_6): δ 169.5, 163.9, 158.3, 150.4, 144.6, 135.6, 135.2, 135.1, 129.9, 128.0, 127.7, 126.9, 113.4, 108.4, 88.0, 86.6, 85.7, 77.1, 73.6, 72.5, 58.8, 55.1, 20.6, 12.4. MALDI-TOF MS: *m/z* 636.5 ($M+Na^+$).

4.1.8. Compound 10b. White solid foam; prepared by the method described for **10a** (yield 89%). ^1H NMR (DMSO-d_6): δ 11.50 (br s, 1H), 7.59 (s, 1H), 7.43–7.23 (m, 9H), 6.93–6.90 (m, 4H), 5.56 (s, 1H), 5.15 (s, 1H), 4.51 (s, 1H), 3.81 (d, *J*=8.4 Hz, 1H), 3.75 (d, *J*=8.4 Hz, 1H), 3.74 (s, 6H), 3.46 (d, *J*=11.5 Hz, 1H), 3.38 (d, *J*=11.5 Hz, 1H), 2.02 (s, 3H), 1.63 (d, *J*=0.9 Hz, 3H). ^{13}C NMR (DMSO-d_6): δ 169.4, 163.8, 158.3, 150.0, 144.5, 135.1, 135.0, 133.8, 129.8, 129.7, 128.1, 127.6, 127.0, 113.4, 109.2, 86.6, 86.5, 86.0, 77.4, 71.7, 70.6, 57.8, 55.1, 20.5, 12.5. MALDI-TOF MS: *m/z* 635.9 ($M+Na^+$). Anal. Calcd for $C_{34}H_{34}N_2O_9 \cdot 1/4H_2O$: C, 65.96; H, 5.62; N, 4.52. Found: C, 65.89; H, 5.55; N, 4.47.

4.1.9. 1-[3-*O*-Acetyl-5-*O*-(4,4′-dimethoxytrityl)-2-*O*,4-*C*-methylene-α-L-ribofuranosyl]-5-methyl-4-(1,2,4-triazol-1-yl)-2-oxypyrimidine (11a). A mixture of compound **10a** (18.5 g, 29.2 mmol) and 1,2,4-triazole (18.6 g, 263 mmol) was suspended in anhydrous acetonitrile (300 mL) and freshly distilled phosphoryl chloride (4.1 mL, 50 mmol) was added. The mixture was cooled in an ice bath and diisopropylethylamine (51 mL, 292.3 mmol) was slowly added under intensive stirring. The mixture was stirred for 2 h at room temperature, diluted with ethyl acetate (300 mL), washed with saturated $NaHCO_3$ (3×300 mL) and brine (250 mL), dried (Na_2SO_4), and concentrated under reduced pressure to give after drying compound **11a** (18.9 g, 97%) as a brownish solid material. RP-HPLC: R_t=12.76 min, $A_{290/260}$=0.235, purity 98% (integration at 260 nm). Analytical sample was obtained after silica gel column chromatography (50–80% v/v EtOAc/hexane, containing 1% of Et_3N) as a white solid foam. ^1H NMR ($CDCl_3$): δ 9.29 (s, 1H), 8.12 (s, 1H), 8.10 (s, 1H), 7.45–7.41 (m, 2H), 7.34–7.24 (m, 7H), 6.88–6.83 (m, 4H), 6.18 (s, 1H), 5.34 (s, 1H), 4.95 (1H, s), 4.07 (d, *J*=9.0 Hz, 1H), 4.01 (d, *J*=9.0 Hz, 1H), 3.80 (s, 6H), 3.57 (d, *J*=11.0 Hz, 1H), 3.46 (d, *J*=11.0 Hz, 1H), 2.55 (s, 3H), 2.05 (s, 3H). ^{13}C NMR ($CDCl_3$): δ 169.1, 158.5, 158.2, 153.5, 153.3, 146.1, 144.9, 144.0, 135.0, 129.8, 127.8, 127.6, 126.9, 113.1, 105.0, 89.05, 88.98, 86.3, 76.8, 73.7, 73.3, 59.1, 55.1, 20.5, 17.4. MALDI-TOF MS: *m/z* 686.7 ($M+Na^+$).

4.1.10. Compound 11b. White solid foam; prepared in 90% yield as described for **11a**. ^1H NMR ($CDCl_3$): δ 9.29 (s, 1H), 8.27 (s, 1H), 8.12 (s, 1H), 7.46–7.24 (m, 9H), 6.89–6.84 (m, 4H), 5.85 (s, 1H), 5.15 (s, 1H), 4.82 (1H, s), 3.91 (d, *J*=8.2 Hz, 1H,), 3.88 (d, *J*=8.2 Hz, 1H), 3.80 (s, 6H), 3.64 (d, *J*=11.2 Hz, 1H), 3.38 (d, *J*=11.2 Hz, 1H), 2.22 (s, 3H), 2.03 (s, 3H,). ^{13}C NMR ($CDCl_3$): δ 169.1, 158.6, 158.4, 153.3, 153.2, 145.4, 145.0, 143.9, 134.8, 129.9, 129.8, 127.9, 127.8, 127.0, 113.2, 106.1, 88.3, 87.4, 86.7, 77.1, 72.1, 70.2, 57.4, 55.1, 20.5, 17.2. MALDI-TOF MS: *m/z* 687.5 ($M+Ma^+$). Anal. Calcd for $C_{36}H_{35}N_5O_8$: C, 64.95; H, 5.30; N, 10.52. Found: C, 64.69; H, 5.26; N, 10.45.

4.1.11. 4-*N*-Benzoyl-1-[5-*O*-(4,4′-dimethoxytrityl)-2-*O*,4-*C*-methylene-α-L-ribofuranosyl]-5-methylcytosine (12a). To a solution of compound **11a** (18.5 g, 27.8 mmol) in MeCN (250 mL) was added concentrated NH_4OH

(200 mL). The mixture was kept overnight at room temperature and the solvents were removed under reduced pressure to give a solid residue. The residue was co-evaporated with anhydrous pyridine (2×200 mL), dissolved in anhydrous pyridine (250 mL), and Bz_2O (19.0 g, 84.0 mmol) was added. After stirring overnight, to the mixture were added MeOH (150 mL) and 2 M NaOH (150 mL). The obtained clear solution was stirred for 1 h and washed with CH_2Cl_2 (2×300 mL). The combined organic phases were excessively washed with saturated $NaHCO_3$ and brine, dried (Na_2SO_4), and concentrated under reduced pressure to a solid residue. Purification by silica gel column chromatography (5–15% v/v EtOAc/CH_2Cl_2, containing 1% of Et_3N) gave compound **12a** (15.2 g, 81%) as a white solid foam.[25]

4.1.12. Compound 12b. White solid foam; prepared as described for **10a** (yield 76%). ^{1}H NMR (DMSO-d_6): δ 13.14 (br s, 1H), 8.20 (m, 2H), 7.79 (s, 1H), 7.57–7.24 (m, 12H), 6.93 (m, 4H), 5.87 (d, J=3.9 Hz, 1H), 5.54 (s, 1H), 4.31 (s, 1H), 4.22 (d, J=4.4 Hz, 1H), 3.81 (d, J=7.9 Hz, 1H), 3.75 (s, 7H), 3.51 (d, J=11.0 Hz, 1H), 3.39 (d, J=11.0 Hz, 1H), 1.80 (s, 3H). ^{13}C NMR (DMSO-d_6): δ 178.3, 159.3, 158.3, 147.0, 144.8, 137.0, 135.4, 135.4, 135.2, 132.6, 129.9, 129.5, 128.3, 128.1, 127.8, 126.9, 113.4, 109.6, 87.8, 87.1, 85.9, 78.7, 71.5, 69.3, 58.6, 55.2, 13.3. MALDI-TOF MS: m/z 697.3 (M+Na$^+$).

4.1.13. 7-(2-*O*-Acetyl-3-*O*-benzyl-4-*C*-methanesulfoxymethyl-5-*O*-methanesulfonyl-β-D-*erythro*-pentofuranosyl)-2-*N*-isobutyrylguanine (15). A mixture of furanose **14**[24] (6.0 g, 11.7 mmol) and 2-*N*-isobutyrylguanine (3.1 g, 14.1 mmol) was suspended in anhydrous MeCN (60 mL) and *N*,*O*-bis(trimethylsilyl)acetamide (5.7 mL, 23.1 mmol) was added. The mixture was stirred overnight whereupon the presence of insoluble residue was still observed. The solvents were removed under reduced pressure and the residue was co-evaporated with anhydrous MeCN (2×50 mL) and suspended in anhydrous MeCN (50 mL). To the mixture was added *N*,*O*-bis(trimethylsilyl)acetamide (2.8 mL, 11.3 mmol). After stirring for 1 h, a clear solution was obtained and $SnCl_4$ (1.5 mL, 12.8 mmol) was added. After stirring for 20 h, the mixture was diluted with EtOAc (100 mL) and saturated $NaHCO_3$ (50 mL). The mixture was filtrated through Celite pad and the Celite was additionally washed with 10% v/v MeOH/EtOAc (50 mL). Organic layer was separated, washed with saturated $NaHCO_3$ (2×100 mL) and brine (50 mL), dried (Na_2SO_4), and concentrated to a solid residue. Purification with silica gel HPLC (0–4% v/v MeOH/CH_2Cl_2) gave compound **15** (2.7 g, 34%) as a white solid foam. ^{1}H NMR ($CDCl_3$): δ 12.07 (br s, 1H), 9.48 (br s, 1H), 7.97 (s, 1H), 7.30 (m, 5H), 6.62 (d, J=5.7 Hz, 1H), 6.32 (s, 1H), 5.33 (d, J=5.8 Hz, 1H), 4.76 (d, J=11.4 Hz, 1H), 4.74 (d, J=11.5 Hz, 1H), 4.68 (d, J=11.4 Hz, 1H), 4.57 (d, J=10.6 Hz, 1H), 4.46 (d, J=11.5 Hz, 1H), 4.44 (d, J=10.5 Hz, 1H), 3.05 (s, 3H), 3.00 (s, 3H), 2.77 (m, 1H), 2.27 (s, 3H), 1.39 (d, J=7.0 Hz, 3H), 1.30 (d, J=6.8 Hz, 3H). ^{13}C NMR ($CDCl_3$): δ 179.7, 170.3, 157.4, 152.2, 147.4, 141.0, 137.1, 128.4, 128.3, 128.1, 110.2, 90.8, 84.7, (77.2, 76.9, 76.6 overlap with $CDCl_3$), 74.1, 68.0, 37.6, 36.7, 36.3, 21.0, 19.0, 18.6. MALDI-TOF MS: m/z 671.8 (M+H$^+$). Anal. Calcd for $C_{26}H_{33}N_5O_{12}S_2$: C, 46.49; H, 4.95; N, 10.43. Found: C, 46.45; H, 4.93; N, 9.90.

4.1.14. 7-(3-*O*-Benzyl-5-*O*-methanesulfonyl-2-*O*,4-*C*-methylene-β-D-ribofuranosyl)-2-*N*-isobutyrylguanine (16). White solid foam; prepared using the method described earlier[24] for the N^9-glycosylated counterpart (yield 89%). ^{1}H NMR ($CDCl_3$): δ 10.17 (br s, 1H), 8.12 (s, 1H), 7.28–7.20 (m, 5H), 6.20 (s, 1H), 4.82 (s, 1H), 4.67 (d, J=11.9 Hz, 1H), 4.60 (d, J=11.9 Hz, 1H), 4.58 (d, J=11.5 Hz, 1H), 4.53 (d, J=11.5 Hz, 1H), 4.21 (s, 1H), 4.15 (d, J=7.9 Hz, 1H), 3.97 (d, J=7.9 Hz, 1H), 3.11 (s, 3H), 2.90 (m, 1H), 1.28 (d, J=6.8 Hz, 3H), 1.22 (d, J=7.0 Hz, 3H). ^{13}C NMR ($CDCl_3$): δ 179.7, 157.4, 152.8, 147.8, 140.0, 136.5, 128.4, 128.1, 127.7, 110.4, 88.3, 85.7, 78.0, 76.1, 72.3, 71.8, 64.2, 37.7, 35.9, 19.0, 18.8. MALDI-TOF MS: m/z 533.6 (M+H$^+$). Anal. Calcd for $C_{23}H_{27}N_5O_8S\cdot 1/6H_2O$: C, 51.49; H, 5.13; N, 13.05. Found: C, 51.46; H, 5.02; N, 12.64.

4.1.15. 7-(5-*O*-Benzoyl-3-*O*-benzyl-2-*O*,4-*C*-methylene-β-D-ribofuranosyl)-2-*N*-isobutyrylguanine (17). White solid foam; prepared using the method described earlier[24] for the N^9-glycosylated counterpart (yield 93%). ^{1}H NMR ($CDCl_3$): δ 10.39 (br s, 1H), 7.99–7.97 (m, 3H), 7.61–7.57 (m, 1H), 7.47–7.43 (m, 2H), 7.23–7.18 (m, 5H), 6.21 (s,1H), 4.84 (s, 1H), 4.80 (d, J=12.7 Hz, 1H), 4.70 (d, J=12.8 Hz, 1H), 4.62 (d, J=11.7 Hz, 1H), 4.48 (d, J=11.7 Hz, 1H), 4.25 (d, J=7.9 Hz, 1H), 4.15 (s, 1H), 4.07 (d, J=7.9 Hz, 1H), 2.96 (m, 1H), 1.25 (d, J=6.8 Hz, 3H), 1.21 (d, J=7.0 Hz, 3H). ^{13}C NMR ($CDCl_3$): δ 179.8, 165.7, 157.5, 152.7, 148.0, 139.7, 136.5, 133.4, 129.4, 129.0, 128.5, 128.3, 128.0, 127.5, 110.5, 88.3, 86.1, 78.0, 76.2, 72.3, 72.1, 59.8, 35.9, 19.0, 18.9. MALDI-TOF MS: m/z 560.0 (M+H$^+$). Anal. Calcd for $C_{29}H_{29}N_5O_7\cdot 1/5H_2O$: C, 61.85; H, 5.26; N, 12.44. Found: C, 61.91; H, 5.25; N, 11.95.

4.1.16. 7-(3-*O*-Benzyl-2-*O*,4-*C*-methylene-β-D-ribofuranosyl)-2-*N*-isobutyrylguanine (18). White crystalline powder; synthesized using the method described earlier[24] for the N^9-glycosylated counterpart; crystallized from MeOH/H_2O (yield 85%). Mp 190–191.5 °C. ^{1}H NMR (DMSO-d_6): δ 12.19 (br s, 1H), 11.57 (br s, 1H), 8.29 (s, 1H), 7.31–7.22 (m, 5H), 6.11 (s,1H), 5.26 (t, J=5.8 Hz, 1H), 4.64 (s, 1H), 4.57 (s, 2H), 4.13 (s, 1H), 3.93 (d, J=7.9 Hz, 1H), 3.85 (d, J=5.8 Hz, 2H), 3.79 (d, J=7.9 Hz, 1H), 2.76 (m, 1H), 1.14–1.11 (m, 6H). ^{13}C NMR (DMSO-d_6): δ 180.1, 157.7, 152.5, 147.4, 140.6, 137.9, 128.3, 127.6, 127.5, 110.5, 88.6, 87.3, 77.8, 76.0, 71.8, 71.3, 56.5, 34.8, 19.0, 18.9. MALDI-TOF MS: m/z 457.1 (M+H$^+$). Anal. Calcd for $C_{29}H_{29}N_5O_7\cdot H_2O$: C, 55.81; H, 5.75; N, 14.79. Found: C, 55.63; H, 5.59; N, 14.69.

4.1.17. 7-(2-*O*,4-*C*-Methylene-β-D-ribofuranosyl)guanine (21). To a solution of compound **18** (540 mg, 1.19 mmol) in MeOH (10 mL) were added Pd/C (10%, 250 mg) and HCO_2NH_4 (0.5 g). The mixture was refluxed until complete consumption of **18** had occurred whereupon formation of insoluble product(s) was observed. Saturated NH_3 in MeOH was added (20 mL) under intensive stirring and the catalyst was filtered off and washed with saturated NH_3 in MeOH (100 mL). The combined filtrates were stirred for 72 h and concentrated to a solid residue. The residue was suspended in MeOH/EtOAc (1:1 v/v, 100 mL) under reflux for 30 min. The mixture was concentrated to ca. half of its volume, and cooled in an ice bath. Insoluble material was filtered off,

washed with EtOAc and Et_2O, and dried in vacuo to give **21** (302 mg, 86%) as a white powder. ^{1}H NMR (DMSO-d_6; low solubility): δ 10.87 (br s, 1H), 8.08 (s, 1H), 6.18 (br s, 2H), 5.94 (s, 1H), 5.59 (br s, 1H), 5.03 (br s, 1H), 4.29 (s, 1H), 4.04 (s, 1H), 3.88 (d, J=7.8 Hz, 1H), 3.79 (m, 2H), 3.70 (d, J=7.7 Hz, 1H). ^{13}C NMR (DMSO-d_6; sugar part): δ 88.7, 87.0, 80.1, 71.1, 68.8, 56.4. MALDI-TOF MS: m/z 296.0 (M+H$^+$).

4.1.18. 7-[5-*O*-(4,4′-Dimethoxytrityl)-2-*O*,4-*C*-methylene-β-D-ribofuranosyl]-2-*N*-dimethylaminomethyleneguanine (22). Compound **21** (250 mg, 0.85 mmol) was dissolved in hot anhydrous DMF (8 mL) and *N*,*N*-dimethylformamide dimethyl acetal (300 μL, 2.26 mmol) was added. The mixture was stirred overnight and H_2O (1 mL) was added. The solvents were removed under reduced pressure to give an oily residue. The residue was co-evaporated with anhydrous pyridine (2×10 mL), dissolved in anhydrous pyridine (5 mL), and DMT-Cl (310 mg, 0.92 mmol) was added. The mixture was stirred for 4 h, diluted with EtOAc (20 mL), washed with saturated $NaHCO_3$ (2×20 mL), dried (Na_2SO_4), and concentrated to a solid residue. Purification by silica gel HPLC (1–4% v/v MeOH/CH_2Cl_2, containing 0.1% of pyridine) gave compound **22** (490 mg, 89%) as a white solid foam. ^{1}H NMR (DMSO-d_6): δ 11.51 (br s, 1H), 8.62, (s, 1H), 8.11 (s, 1H), 7.46–7.28 (m, 9H), 6.91 (m, 4H), 6.10 (s, 1H), 5.71 (d, J=4.4 Hz, 1H), 4.41 (s, 1H), 4.20 (d, J=4.4 Hz, 1H), 3.89 (d, J=7.9 Hz, 1H), 3.86 (d, J=7.9 Hz, 1H), 3.75 (s, 6H), 3.56 (d, J=11.0 Hz, 1H), 3.33 (d, J=11.0 Hz, 1H), 3.15 (s, 3H), 3.02 (s, 3H). ^{13}C NMR (DMSO-d_6): δ 159.5, 158.2, 157.9, 156.9, 155.2, 144.8, 139.6, 135.5, 135.3, 129.9, 129.8, 128.0, 127.8, 126.9, 113.4, 109.9, 87.3, 85.6, 80.2, 71.6, 69.5, 59.6, 55.2, 40.6, 34.7. MALDI-TOF MS: m/z 675.7 (M+Na$^+$).

4.1.19. 7-[3-*O*-Cyanoethoxy(diisopropylamino)phosphinoxy)-5-*O*-(4,4′-dimethoxytrityl)-2-*O*,4-*C*-methylene-β-D-ribofuranosyl]-2-*N*-dimethylaminomethyleneguanine (23). To a solution of compound **22** (415 mg, 0.64 mmol) in anhydrous CH_2Cl_2 (3 mL) were added 0.75 M solution of 4,5-dicyanoimidazole (700 μL, 0.53 mmol) in CH_3CN and 2-cyanoethyl-*N*,*N*,*N*′,*N*′-tetraisopropyl phosphordiamidite (230 μL, 0.72 mmol). The mixture was stirred overnight, diluted with EtOAc (25 mL), and washed with saturated $NaHCO_3$ (2×25 mL) and brine (25 mL). The organic layer was dried (Na_2SO_4) and concentrated to a white solid residue. The residue was dissolved in anhydrous CH_2Cl_2 (5 mL) and pentane (100 mL) was added under intensive stirring. The precipitate formed was collected by filtration, washed with pentane, and dried in vacuo to give compound **23** (498 mg, 92%) as a white amorphous powder consisting of two stereoisomers. RP-HPLC: R_t=15.05 min, $A_{290/260}$=2.54. MALDI-TOF MS: m/z 791.2 (M−N^{i}Pr$_2$+OH+Na$^+$). ^{31}P NMR (DMSO-d_6): δ 149.20, 147.98.

Compound **20**. ^{31}P NMR (DMSO-d_6): δ 148.96, 148.70.

4.2. Oligonucleotide synthesis

All oligonucleotides were synthesized in 0.2 μmol scales on Expedite DNA synthesizer using the phosphoramidite method. Standard protocols recommended by the manufacturer were used for commercial DNA amidites. For all LNA amidites coupling times and times of oxidation were extended to 500 and 30 s, respectively. After oligomerization, the solid support bound oligonucleotides were transferred into 1.5 mL reaction tubes and treated with concentrated NH_4OH for 6 h at 60 °C. Oligonucleotide **46** (phosphoramidite **20** used) was subsequently treated with 30% $MeNH_2$ for 2 h at 60 °C. The solvents were removed under reduced pressure and target oligonucleotides were purified by RP-HPLC. Structures of the oligonucleotides were verified by MALDI-TOF mass spectra recorded in negative ion mode using picolinic acid as the matrix (results shown in Table 3).

Table 3. The results of MALDI-TOF analysis

Oligonucleotide	(M−H)$^-$	
	Calcd	Found
24	4385.8	4380.1
25	4385.8	4381.3
26	4385.8	4385.2
27	4581.8	4576.6
28	4581.8	4583.0
29	4385.8	4386.0
30	4385.8	4383.9
31	4385.8	4384.0
32	4385.8	4384.7
33	4515.7	4513.1
34	4463.7	4459.4
35	4435.7	4435.4
36	4379.7	4376.8
37	4411.8	4405.1
38	4411.8	4407.8
39	4411.8	4410.6
40	9259.0	9264.0
41	9150.8	9147.0
42	4417.7	4414.8
43	2672.7	2972.8
44	2681.8	2681.9
45	2697.5	2698.9
46	2697.5	2697.9

4.3. Thermal denaturation studies

The samples of model triplexes and duplexes were obtained after mixing the equal molar amounts of complementary oligonucleotides and buffers (final volumes 0.5 mL). The buffer and concentration conditions are described in the footnotes to Tables 1 and 2. To ensure triplex formation, the samples were kept for 12 h at 4 °C prior to melting experiments. Melting temperature measurements were carried out on a Perkin–Elmer UV-spectrometer equipped with a PTP-6 Peltier temperature controller. The optical density of samples was monitored at 260 nm while raising the temperature from 20 to 95 °C at a rate of 1 °C/min. The T_m values were determined as the maxima of the first derivatives of the melting curves obtained.

References and notes

1. Felsenfeld, G.; Davies, D. R.; Rich, A. *J. Am. Chem. Soc.* **1957**, *79*, 2023–2024.
2. Giovannangeli, C.; Helene, C. *Curr. Opin. Mol. Ther.* **2000**, *2*, 288–296.
3. Uil, T. G.; Haisma, H. J.; Rots, M. G. *Nucleic Acids Res.* **2003**, *31*, 6603–6614.

4. Soyfer, V. N.; Potoman, V. N. *Triple-helical Nucleic Acids*; Springer: New York, NY, 1996.
5. Beal, P. A.; Dervan, P. B. *Science* **1991**, *251*, 1360–1363.
6. Goni, J. R.; de la Cruz, X.; Orozco, M. *Nucleic Acids Res.* **2004**, *32*, 354–360.
7. Kuan, J. Y.; Glazer, P. M. *Methods Mol. Biol.* **2004**, *262*, 173–194.
8. Faria, M.; Giovannangeli, C. *J. Gene Med.* **2001**, *3*, 299–310.
9. Buchini, S.; Leumann, C. J. *Curr. Opin. Chem. Biol.* **2003**, *7*, 717–726.
10. Nielsen, P. E.; Egholm, M.; Berg, R. H.; Buchardt, O. *Science* **1991**, *254*, 1497–1500.
11. Egholm, M.; Buchardt, O.; Chistensen, L.; Behrens, C.; Freier, S. M.; Driver, D. A.; Berg, R. H.; Kim, S. K.; Norden, B.; Nielsen, P. E. *Nature* **1993**, *365*, 566–568.
12. Nielsen, P. E. *Curr. Med. Chem.* **2001**, *8*, 545–550.
13. Cherny, D. Y.; Belotserkovskii, B. P.; Frank-Kamenetskii, M. D.; Egholm, M.; Buchardt, O.; Berg, R. H.; Nielsen, P. E. *Proc. Natl. Acad. Sci. U.S.A.* **1993**, *90*, 1667–1670.
14. Cutrona, G.; Carpaneto, E. M.; Ulivi, M.; Roncella, S.; Landt, O.; Ferrarini, M.; Boffa, L. C. *Nature Biotechnol.* **2000**, *18*, 300–303.
15. Gryaznov, S. M.; Chen, J.-K. *J. Am. Chem. Soc.* **1994**, *116*, 3143–3144.
16. Escude, C.; Giovannangeli, C.; Sun, J. S.; Lloyd, D. H.; Chen, J. K.; Gryaznov, S. M.; Garestier, T.; Helene, C. *Proc. Natl. Acad. Sci. U.S.A.* **1996**, *93*, 4365–4369.
17. Skorski, T.; Perrotti, D.; Nieborowska-Skorska, M.; Gryaznov, S.; Calabretta, B. *Proc. Natl. Acad. Sci. U.S.A.* **1997**, *94*, 3966–3971.
18. Tereshko, V.; Gryaznov, S.; Egli, M. *J. Am. Chem. Soc.* **1998**, *120*, 269–283.
19. Obika, S.; Nanbu, D.; Hari, Y.; Morio, K.; In, Y.; Ishida, T.; Imanishi, T. *Tetrahedron Lett.* **1997**, *38*, 8735–8738.
20. Morita, K.; Takagi, M.; Hasegawa, C.; Masakatsu, K.; Tsutsumi, S.; Sone, J.; Ishikawa, T.; Imanishi, T.; Koizumi, M. *Bioorg. Med. Chem.* **2003**, *11*, 2211–2226.
21. Obika, S. *Chem. Pharm. Bull.* **2004**, *52*, 1399–1404.
22. Koizumi, M.; Morita, K.; Daigo, M.; Tsutsumi, S.; Koji, A.; Obika, S.; Imanishi, T. *Nucleic Acids Res.* **2003**, *31*, 3267–3273.
23. Sørensen, J. J.; Nielsen, J. T.; Pedersen, M. *Nucleic Acids Res.* **2004**, *32*, 6078–6085.
24. Koshkin, A. A.; Fensholdt, J.; Pfundheller, H. M.; Lomholt, C. *J. Org. Chem.* **2001**, *66*, 8504–8512.
25. Sørensen, M. D.; Kværnø, L.; Bryld, T.; Håkansson, A. E.; Verbeure, B.; Gaubert, G.; Herdewijn, P.; Wengel, J. *J. Am. Chem. Soc.* **2002**, *124*, 2164–2176.
26. Håkansson, A. E.; Koshkin, A. A.; Sørensen, M. D.; Wengel, J. *J. Org. Chem.* **2000**, *65*, 5161–5166.
27. Nielsen, K. M. E.; Pedersen, M.; Håkansson, A. E.; Wengel, J.; Jacobsen, J. P. *Chem.—Eur. J.* **2002**, *8*, 3001–3009.
28. Hunziker, J.; Priestley, E. S.; Brunar, H.; Dervan, P. B. *J. Am. Chem. Soc.* **1995**, *117*, 2661–2662.
29. Brunar, H.; Dervan, P. B. *Nucleic Acids Res.* **1996**, *24*, 1987–1991.
30. Vorbrüggen, H.; Höfle, G. *Chem. Ber.* **1981**, *114*, 1256–1268.
31. Pedersen, D. S.; Rosenbohm, C.; Koch, T. *Synthesis* **2002**, 802–808.
32. Lee, J. S.; Woodsworth, M. L.; Latimer, L. J.; Morgan, A. R. *Nucleic Acids Res.* **1984**, *12*, 6603–6614.
33. Obika, S.; Uneda, T.; Sugimoto, T.; Nanbu, D.; Minami, T.; Doi, T.; Imanishi, T. *Bioorg. Med. Chem.* **2001**, *9*, 1001–1011.
34. Koshkin, A. A.; Singh, S. K.; Nielsen, P.; Rajwanshi, V. K.; Kumar, R.; Meldgaard, M.; Olsen, C. E.; Wengel, J. *Tetrahedron* **1998**, *54*, 3607–3630.
35. Divakar, K. J.; Reese, C. B. *J. Chem. Soc., Perkin Trans. 1* **1982**, 1171–1176.
36. Seela, F.; Leonard, P. *Helv. Chim. Acta* **1996**, *79*, 477–487.
37. Rosenbohm, C.; Pedersen, D. S.; Frieden, M.; Jensen, F. R.; Arent, S.; Larsen, S.; Koch, T. *Bioorg. Med. Chem.* **2004**, *12*, 2385–2396.
38. Caruthers, M. H. *Acc. Chem. Res.* **1991**, *24*, 278–284.
39. McBride, L. J.; Kierzek, R.; Beaucage, S. L.; Caruthers, M. H. *J. Am. Chem. Soc.* **1986**, *108*, 2040–2048.
40. Sun, B.-W.; Babu, B. R.; Sørensen, M. D.; Zakrzewska, K.; Wengel, J.; Sun, J.-S. *Biochemistry* **2004**, *43*, 4160–4169.
41. Alberti, P.; Arimondo, P. B.; Mergny, J.-L.; Garestier, T.; Hélène, C.; Sun, J.-S. *Nucleic Acids Res.* **2002**, *30*, 5407–5415.